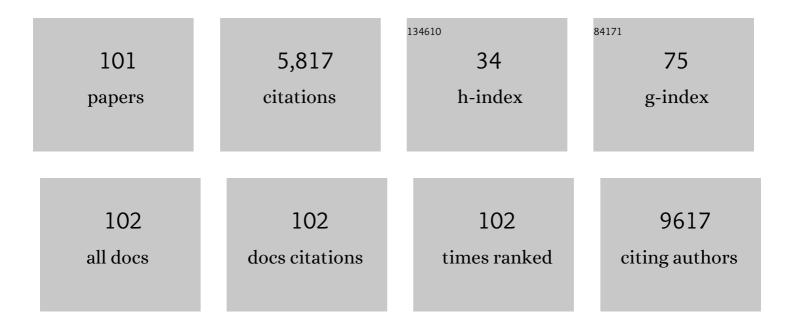
## List of Publications by Year in descending order

Source: https://exaly.com/author-pdf/698161/publications.pdf Version: 2024-02-01



 $\mathbf{v}_{i}$ 

#	Article	IF	CITATIONS
1	Substrate tuned reconstructed polymerization of naphthalocyanine on Ag(110). Chinese Physics B, 2022, 31, 018202.	0.7	0
2	Se-concentration dependent superstructure transformations of CuSe monolayer on Cu(111) substrate. 2D Materials, 2022, 9, 015017.	2.0	5
3	Intrinsically Honeycombâ€Patterned Hydrogenated Graphene. Small, 2022, 18, e2102687. Observation of an Incommensurate Charge Density Wave in Monolayer <mml:math< td=""><td>5.2</td><td>3</td></mml:math<>	5.2	3
4	xmlns:mml="http://www.w3.org/1998/Math/Math/ML" display="inline"> <mml:mrow><mml:msub><mml:mrow><mml:mi>TiSe</mml:mi></mml:mrow><mml:mrow><n stretchy="false"&gt;(<mml:mn>1</mml:mn>111111</n </mml:mrow></mml:msub></mml:mrow>	ıml;mn>2∢ Tj ETQq0 (	0 0 rgBT /Ove
5	2022, 128, 026401. 5f Covalency Synergistically Boosting Oxygen Evolution of UCoO <sub>4</sub> Catalyst. Journal of the American Chemical Society, 2022, 144, 416-423.	6.6	48
6	Line defects in monolayer TiSe2 with adsorption of Pt atoms potentially enable excellent catalytic activity. Nano Research, 2022, 15, 4687-4692.	5.8	9
7	Intrinsically patterned corrals in monolayer Ag5Se2 and selective molecular co-adsorption. Nano Research, 2022, 15, 6730-6735.	5.8	3
8	Chirality locking charge density waves in a chiral crystal. Nature Communications, 2022, 13, .	5.8	12
9	Growth of LaCoO <sub>3</sub> crystals in molten salt: effects of synthesis conditions. CrystEngComm, 2021, 23, 671-677.	1.3	5
10	Edge- and strain-induced band bending in bilayer-monolayer Pb2Se3 heterostructures. Chinese Physics B, 2021, 30, 018105.	0.7	7
11	The As-surface of an iron-based superconductor CaKFe4As4. Nano Research, 2021, 14, 3921-3925.	5.8	6
12	Intercalation of germanium oxide beneath large-area and high-quality epitaxial graphene on Ir(111) substrate*. Chinese Physics B, 2021, 30, 048102.	0.7	7
13	Three-dimensional microstructural characterization of solid oxide electrolysis cell with Ce0.8Gd0.2O2-infiltrated Ni/YSZ electrode using focused ion beam-scanning electron microscopy. Journal of Solid State Electrochemistry, 2021, 25, 1633-1644.	1.2	10
14	Honeycomb AgSe Monolayer Nanosheets for Studying Two-dimensional Dirac Nodal Line Fermions. ACS Applied Nano Materials, 2021, 4, 8845-8850.	2.4	13
15	Novel two-dimensional transition metal chalcogenides created by epitaxial growth. Science China: Physics, Mechanics and Astronomy, 2021, 64, 1.	2.0	3
16	A Tunable Amorphous Heteronuclear Iron and Cobalt Imidazolate Framework Analogue for Efficient Oxygen Evolution Reactions. European Journal of Inorganic Chemistry, 2021, 2021, 702-707.	1.0	7
17	Controllable fabrication and photocatalytic performance of nanoscale single-layer MoSe <sub>2</sub> islands with substantial edges on an Ag(111) substrate. Nanoscale, 2021, 13, 19165-19171.	2.8	5
18	Two distinct superconducting states controlled by orientations of local wrinkles in LiFeAs. Nature	5.8	16

Communications, 2021, 12, 6312.

#	Article	IF	CITATIONS
19	Rational Design of Two-Layer Fe-Doped PrBa <sub>0.8</sub> Ca <sub>0.2</sub> Co <sub>2</sub> O <sub>6â~îî</sub> Double Perovskite Oxides for High-Performance Fuel Cell Cathodes. Journal of Physical Chemistry C, 2021, 125, 26448-26459.	1.5	5
20	Direct growth of wafer-scale highly oriented graphene on sapphire. Science Advances, 2021, 7, eabk0115.	4.7	43
21	On-Surface Synthesis and Characterization of Polythiophene Chains. Journal of Physical Chemistry C, 2020, 124, 764-768.	1.5	6
22	Layer-by-Layer Epitaxy of Porphyrinâ^'Ligand Fe(II)-Fe(III) Nanoarchitectures for Advanced Metal–Organic Framework Growth. ACS Applied Nano Materials, 2020, 3, 11752-11759.	2.4	12
23	Insulating SiO <sub>2</sub> under Centimeter-Scale, Single-Crystal Graphene Enables Electronic-Device Fabrication. Nano Letters, 2020, 20, 8584-8591.	4.5	19
24	Localized spin-orbit polaron in magnetic Weyl semimetal Co3Sn2S2. Nature Communications, 2020, 11, 5613.	5.8	53
25	Epitaxial fabrication of monolayer copper arsenide on Cu(111)*. Chinese Physics B, 2020, 29, 077301.	0.7	5
26	Force-Activated Isomerization of a Single Molecule. Journal of the American Chemical Society, 2020, 142, 10673-10680.	6.6	16
27	Sizable Band Gap in Epitaxial Bilayer Graphene Induced by Silicene Intercalation. Nano Letters, 2020, 20, 2674-2680.	4.5	23
28	Air‣table Monolayer Cu <sub>2</sub> Se Exhibits a Purely Thermal Structural Phase Transition. Advanced Materials, 2020, 32, e1908314.	11.1	26
29	Experimental Synthesis of Strained Monolayer Silver Arsenide on Ag(111) Substrates. Chinese Physics Letters, 2020, 37, 068103.	1.3	10
30	Unexpected Roles of Alkali-Metal Cations in the Assembly of Low-Valent Uranium Sulfate Molecular Complexes. Inorganic Chemistry, 2020, 59, 2348-2357.	1.9	11
31	Epitaxial synthesis and electronic properties of monolayer Pd <sub>2</sub> Se <sub>3</sub> *. Chinese Physics B, 2020, 29, 098102.	0.7	7
32	Direct probing of imperfection-induced electrical degradation in millimeter-scale graphene on SiO <sub>2</sub> substrates. 2D Materials, 2019, 6, 045033.	2.0	2
33	Centimeter-scale, single-crystalline, AB-stacked bilayer graphene on insulating substrates. 2D Materials, 2019, 6, 045044.	2.0	11
34	Real-space observation on standing configurations of phenylacetylene on Cu (111) by scanning probe microscopy*. Chinese Physics B, 2019, 28, 066801.	0.7	2
35	Epitaxial fabrication of two-dimensional TiTe2 monolayer on Au(111) substrate with Te as buffer layer. Chinese Physics B, 2019, 28, 056801.	0.7	6
36	Interaction of two symmetric monovacancy defects in graphene. Chinese Physics B, 2019, 28, 046801.	0.7	2

#	Article	IF	CITATIONS
37	Spontaneous Formation of 1D Pattern in Monolayer VSe <sub>2</sub> with Dispersive Adsorption of Pt Atoms for HER Catalysis. Nano Letters, 2019, 19, 4897-4903.	4.5	42
38	Study of the relationship between the local geometric structure and the stability of La0.6Sr0.4MnO3â~δ and La0.6Sr0.4FeO3â~δ electrodes. Nuclear Science and Techniques/Hewuli, 2019, 30, 1.	1.3	3
39	Epitaxial Growth of Honeycomb Monolayer CuSe with Dirac Nodal Line Fermions. Advanced Materials, 2018, 30, e1707055.	11.1	110
40	Recovery of edge states of graphene nanoislands on an iridium substrate by silicon intercalation. Nano Research, 2018, 11, 3722-3729.	5.8	10
41	Controllable Density of Atomic Bromine in a Two-Dimensional Hydrogen Bond Network. Journal of Physical Chemistry C, 2018, 122, 25681-25684.	1.5	6
42	Construction of bilayer PdSe2 on epitaxial graphene. Nano Research, 2018, 11, 5858-5865.	5.8	84
43	Epitaxial growth and physical properties of 2D materials beyond graphene: from monatomic materials to binary compounds. Chemical Society Reviews, 2018, 47, 6073-6100.	18.7	97
44	Modification of the Potential Landscape of Molecular Rotors on Au(111) by the Presence of an STM Tip. Nano Letters, 2018, 18, 4704-4709.	4.5	21
45	Tuning the morphology of chevron-type graphene nanoribbons by choice of annealing temperature. Nano Research, 2018, 11, 6190-6196.	5.8	20
46	High quality PdTe2 thin films grown by molecular beam epitaxy. Chinese Physics B, 2018, 27, 086804.	0.7	39
47	Identifying and Visualizing the Edge Terminations of Single-Layer MoSe <sub>2</sub> Island Epitaxially Grown on Au(111). ACS Nano, 2017, 11, 1689-1695.	7.3	48
48	Intrinsically patterned two-dimensional materials for selective adsorption of molecules andÂnanoclusters. Nature Materials, 2017, 16, 717-721.	13.3	150
49	Construction of Two-Dimensional Chiral Networks through Atomic Bromine on Surfaces. Journal of Physical Chemistry Letters, 2017, 8, 326-331.	2.1	33
50	Sulfur-doped graphene nanoribbons with a sequence of distinct band gaps. Nano Research, 2017, 10, 3377-3384.	5.8	44
51	Synthesis of palladium nanoparticles on TiO <sub>2</sub> (110) using a beta-diketonate precursor. Physical Chemistry Chemical Physics, 2015, 17, 6470-6477.	1.3	7
52	Uniform Doping of Titanium in Hematite Nanorods for Efficient Photoelectrochemical Water Splitting. ACS Applied Materials & Interfaces, 2015, 7, 14072-14078.	4.0	43
53	Construction of single-crystalline supramolecular networks of perchlorinated hexa- <i>peri</i> -hexabenzocoronene on Au(111). Journal of Chemical Physics, 2015, 142, 101911.	1.2	13
54	High quality sub-monolayer, monolayer, and bilayer graphene on Ru(0001). Chinese Physics B, 2014, 23, 098101.	0.7	8

#	Article	IF	CITATIONS
55	Effects of graphene defects on Co cluster nucleation and intercalation. Chinese Physics B, 2014, 23, 088108.	0.7	3
56	The evaluation of van der Waals interaction in the oriented-attachment growth of nanotubes. Materials Research Society Symposia Proceedings, 2014, 1705, 1.	0.1	0
57	Direct visualization of atomically precise nitrogen-doped graphene nanoribbons. Applied Physics Letters, 2014, 105, .	1.5	82
58	Quantitative evaluation of Coulombic interactions in the oriented-attachment growth of nanotubes. Analyst, The, 2014, 139, 371-374.	1.7	12
59	Construction of 2D Atomic Crystals on Transition Metal Surfaces: Graphene, Silicene, and Hafnene. Small, 2014, 10, 2215-2225.	5.2	91
60	Commensurate–incommensurate transition in graphene on hexagonal boron nitride. Nature Physics, 2014, 10, 451-456.	6.5	737
61	Recent progress in degradation and stabilization of organic solar cells. Journal of Power Sources, 2014, 264, 168-183.	4.0	136
62	Separation-dependence evolution of inter-particle interaction in the oriented-attachment growth of nanorods: a case of hexagonal nanocrystals. Analyst, The, 2014, 139, 3393-3397.	1.7	2
63	Dimerization Induced Deprotonation of Water on RuO <sub>2</sub> (110). Journal of Physical Chemistry Letters, 2014, 5, 3445-3450.	2.1	47
64	Electrochemical devices with optimized gas tightness for the diffusivity measurement in fuel cells. International Journal of Hydrogen Energy, 2014, 39, 2334-2339.	3.8	5
65	Coulombic interaction in the colloidal oriented-attachment growth of tetragonal nanorods. Chinese Physics B, 2014, 23, 056103.	0.7	3
66	An electrochemical device for three-dimensional (3D) diffusivity measurement in fuel cells. Nano Energy, 2013, 2, 1004-1009.	8.2	19
67	Gas transport in porous electrodes of solid oxide fuel cells: A review on diffusion and diffusivity measurement. Journal of Power Sources, 2013, 237, 64-73.	4.0	73
68	Interaction of CO2 with oxygen adatoms on rutile TiO2(110). Physical Chemistry Chemical Physics, 2013, 15, 6190.	1.3	13
69	Site-Specific Imaging of Elemental Steps in Dehydration of Diols on TiO <sub>2</sub> (110). ACS Nano, 2013, 7, 10414-10423.	7.3	20
70	The evaluation of Coulombic interaction in the oriented-attachment growth of colloidal nanorods. Analyst, The, 2012, 137, 4917.	1.7	21
71	Structure and Dynamics of CO <sub>2</sub> on Rutile TiO <sub>2</sub> (110)-1×1. Journal of Physical Chemistry C, 2012, 116, 26322-26334.	1.5	60
72	Stabilizing Gold Adatoms by Thiophenyl Derivatives: A Possible Route toward Metal Redispersion. Journal of the American Chemical Society, 2012, 134, 11161-11167.	6.6	16

#	Article	IF	CITATIONS
73	OH Group Dynamics of 1,3-Propanediol on TiO2(110). Journal of Physical Chemistry Letters, 2012, 3, 3257-3263.	2.1	16
74	Site- and Configuration-Selective Anchoring of Iron–Phthalocyanine on the Step Edges of Au(111) Surface. Journal of Physical Chemistry C, 2011, 115, 10791-10796.	1.5	31
75	Role of the V2O3(0001) Defect Structure in the Adsorption of Au Adatoms. Journal of Physical Chemistry C, 2011, 115, 3404-3409.	1.5	2
76	Surface reconstruction transition of metals induced by molecular adsorption. Physical Review B, 2011, 83, .	1.1	26
77	Characterizing low-coordinated atoms at the periphery of MgO-supported Au islands using scanning tunneling microscopy and electronic structure calculations. Physical Review B, 2010, 81, .	1.1	67
78	Charge-Mediated Adsorption Behavior of CO on MgO-Supported Au Clusters. Journal of the American Chemical Society, 2010, 132, 7745-7749.	6.6	112
79	CO Adsorption on Thin MgO Films and Single Au Adatoms: A Scanning Tunneling Microscopy Study. Journal of Physical Chemistry C, 2010, 114, 8997-9001.	1.5	22
80	Quantum Well States in Two-Dimensional Gold Clusters on MgO Thin Films. Physical Review Letters, 2009, 102, 206801.	2.9	128
81	Charge-induced formation of linear Au clusters on thin MgO films: Scanning tunneling microscopy and density-functional theory study. Physical Review B, 2008, 78, .	1.1	64
82	Self-Assembly of MgPc Molecules on Polar FeO Thin Films. Journal of Physical Chemistry C, 2008, 112, 15325-15328.	1.5	34
83	Microwave Absorption of Single-Walled Carbon Nanotubes/Soluble Cross-Linked Polyurethane Composites. Journal of Physical Chemistry C, 2007, 111, 13696-13700.	1.5	324
84	Nucleation and Growth of Gold on MgO Thin Films:  A Combined STM and Luminescence Study. Journal of Physical Chemistry C, 2007, 111, 10528-10533.	1.5	39
85	Epitaxial Growth of Iron Phthalocyanine at the Initial Stage on Au(111) Surface. Journal of Physical Chemistry C, 2007, 111, 2656-2660.	1.5	124
86	Site-Specific Kondo Effect at Ambient Temperatures in Iron-Based Molecules. Physical Review Letters, 2007, 99, 106402.	2.9	242
87	Observation of Structural and Conductance Transition of Rotaxane Molecules at a Submolecular Scale. Advanced Functional Materials, 2007, 17, 770-776.	7.8	37
88	Structural evolution at the initial growth stage of perylene on Au(111). Surface Science, 2007, 601, 3179-3185.	0.8	17
89	The influence of single-walled carbon nanotube structure on the electromagnetic interference shielding efficiency of its epoxy composites. Carbon, 2007, 45, 1614-1621.	5.4	524
90	Electromagnetic Interference (EMI) Shielding of Single-Walled Carbon Nanotube Epoxy Composites. Nano Letters, 2006, 6, 1141-1145.	4.5	1,106

#	Article	IF	CITATIONS
91	Manipulation and four-probe analysis of nanowires in UHV by application of four tunneling microscope tips: a new method for the investigation of electrical transport through nanowires. Surface and Interface Analysis, 2006, 38, 1096-1102.	0.8	11
92	Role of Lateral Alkyl Chains in Modulation of Molecular Structures on Metal Surfaces. Physical Review Letters, 2006, 96, 226101.	2.9	51
93	Understanding and controlling the weakly interacting interface inperyleneâ^•Ag(110). Physical Review B, 2006, 73, .	1.1	29
94	Intrinsic current-voltage properties of nanowires with four-probe scanning tunneling microscopy: A conductance transition of ZnO nanowire. Applied Physics Letters, 2006, 89, 043103.	1.5	72
95	Selective Analysis of Molecular States by Functionalized Scanning Tunneling Microscopy Tips. Physical Review Letters, 2006, 96, 156102.	2.9	44
96	Surface crystallization effects on the optical and electric properties of CdS nanorods. Nanotechnology, 2005, 16, 2402-2406.	1.3	20
97	Stable, Reproducible Nanorecording on Rotaxane Thin Films. Journal of the American Chemical Society, 2005, 127, 15338-15339.	6.6	77
98	Crystalline Thin Films Formed by Supramolecular Assembly for Ultrahigh-Density Data Storage. Advanced Materials, 2004, 16, 2018-2021.	11.1	27
99	Patterns formed on the dimer vacancy array of Si(100) by self-assembly. Nanotechnology, 2002, 13, 729-732.	1.3	6
100	Direct observation of surface structure of d-alanine and d-/l-valine crystals by atomic force microscopy and comparison with X-ray diffraction analysis. Surface Science, 2002, 512, L379-L384.	0.8	15
101	MgO intercalation and crystallization between epitaxial graphene and Ru(0001). Rare Metals, 0, , 1.	3.6	5